

PART OF A SPECIAL ISSUE ON FUNCTIONAL–STRUCTURAL PLANT GROWTH MODELLING  
**Structural and functional changes in coffee trees after 4 years under free air  
CO<sub>2</sub> enrichment**

**Miroslava Rakocevic<sup>1,2,\*</sup>, Rafael Vasconcelos Ribeiro<sup>2</sup>, Paulo Eduardo Ribeiro Marchiori<sup>3</sup>,  
Heloisa Ferreira Filizola<sup>4</sup> and Eunice Reis Batista<sup>4</sup>**

<sup>1</sup>Embrapa Agricultural Informatics, Av. André Tosello 209, PO Box 6041, 13083–886 Campinas-SP, Brazil, <sup>2</sup>University of Campinas (UNICAMP), Institute of Biology, Department of Plant Biology, R. Monteiro Lobato, 255 – Cidade Universitária, 13083–862 Campinas-SP, Brazil, <sup>3</sup>Federal University of Lavras (UFLA), Department of Biology, Câmpus Universitário, PO Box 3037, 37200-000 Lavras-MG, Brazil and <sup>4</sup>Embrapa Environment, Rodovia SP 340, km 127.5, 13820-000 Jaguariúna-SP, Brazil

\*For correspondence. E-mail [mimarako@unicamp.br](mailto:mimarako@unicamp.br)

Received: 27 May 2017 Returned for revision: 22 November 2017 Editorial decision: 11 January 2018 Accepted: 17 January 2018  
Published electronically 13 February 2018

- **Background and Aims** Climate forecasts suggest that [CO<sub>2</sub>] in the atmosphere will continue to increase. Structural and ecophysiological responses to elevated air [CO<sub>2</sub>] (e[CO<sub>2</sub>]) in tree species are contradictory due to species-dependent responses and relatively short-term experiments. It was hypothesized that long-term exposure (4 year) to e[CO<sub>2</sub>] would change canopy structure and function of *Coffea arabica* trees.
- **Methods** Coffee plants were grown in a FACE (free air CO<sub>2</sub> enrichment) facility under two air [CO<sub>2</sub>]: actual and elevated (actual + approx. 200 µL CO<sub>2</sub> L<sup>-1</sup>). Plants were codified following the VPlants methodology to obtain coffee mock-ups. Plant canopies were separated into three 50 cm thick layers over a vertical profile to evaluate their structure and photosynthesis, using functional–structural plant modelling.
- **Key Results** Leaf area was strongly reduced on the bottom and upper canopy layers, and increased soil carbon concentration suggested changes in carbon partitioning of coffee trees under e[CO<sub>2</sub>]. Increased air [CO<sub>2</sub>] stimulated stomatal conductance and leaf photosynthesis at the middle and upper canopy layers, increasing water-use efficiency. Under e[CO<sub>2</sub>], plants showed reduced diameter of the second-order axes and higher investment in the youngest third to fifth-order axes.
- **Conclusions** The responses of Arabica coffee grown under long-term exposure to e[CO<sub>2</sub>] integrated structural and functional modifications, which balanced leaf area loss through improvements in leaf and whole-plant photosynthesis.

**Key words:** *Coffea arabica*, FACE, leaf area, metamer, photosynthetic light response curve, plant architecture, stomatal conductance, transpiration, vertical profile, VPlants, whole-plant photosynthesis.

## INTRODUCTION

Intensive farming and industry have emitted significant amounts of gases that increase the greenhouse effect (reviewed by Hillel and Rosenzweig, 2012), such as carbon dioxide (CO<sub>2</sub>) and methane (CH<sub>4</sub>). Since the mid-20th century, the air warming is perceived as an extremely likely consequence of human activities. In fact, air [CO<sub>2</sub>] has increased at rates from 1 to 1.8 µL CO<sub>2</sub> L<sup>-1</sup> air year<sup>-1</sup>, and ecosystem responses to rising air [CO<sub>2</sub>] are major sources of uncertainty in climate change projections (Medlyn *et al.*, 2015). Artificial facilities such as growth chambers and open top chambers (Kimball, 1992) give us the opportunity to study mostly short-term responses to elevated air [CO<sub>2</sub>], here referred to as e[CO<sub>2</sub>]. On the other hand, free air CO<sub>2</sub> enrichment (FACE) systems have been developed to support mid- to long-term studies of physiological responses to e[CO<sub>2</sub>], such as of sorghum (Cousins *et al.*, 2001), soybean (Bishop *et al.*, 2015), wheat (Bunce, 2017), tree species (Koike *et al.*, 2015) and even ecological systems (Macháčková, 2010).

Understanding structural and ecophysiological responses to e[CO<sub>2</sub>] in tree species is complex, due to species-dependent

responses and relatively short-term experiments when compared with the natural tree life cycle. Generally, the initial ecophysiological responses to e[CO<sub>2</sub>] on the leaf scale are enhancement of CO<sub>2</sub> assimilation and a decrease in stomatal conductance ( $g_s$ ; Leakey *et al.*, 2009), with all other effects observed in plants being derived from these two fundamental responses (Ainsworth and Rogers, 2007). Because e[CO<sub>2</sub>] reduces transpiration through partial stomatal closure, while it increases photosynthesis, improvement of water-use efficiency has been reported in many plant species (Xu *et al.*, 2016). Curiously, increases in  $g_s$  were found in pigeon pea plants under e[CO<sub>2</sub>] (Sreeharsha *et al.*, 2015), and in such cases increased photosynthesis would be the key underlying response leading to increases in water-use efficiency. Regarding photosynthesis, the stimulatory effect of e[CO<sub>2</sub>] is related to decreases in photorespiration by reducing the oxygenase activity of Rubisco (Cousins *et al.*, 2001). Various plant species grown under e[CO<sub>2</sub>] show a reduction in the intensity of their initial responses after long-term exposure (Long *et al.*, 2004). Such downregulation could be manifested as reductions in  $g_s$  (Bunce, 2001) and photosynthesis, indicating acclimation of leaf gas exchange caused by sugar accumulation

due to low sink strength (Tuba and Lichtenthaler, 2007). Such photosynthetic downregulation might also represent a shift in carbon partitioning and use under e[CO<sub>2</sub>] (Kubiske et al., 2002; Reddy and Zhao, 2005; Jin et al., 2016).

Under e[CO<sub>2</sub>], architectural and morphological modifications are slower, more conservative and consequently more scarce when compared with changes in leaf gas exchange. The effects of e[CO<sub>2</sub>] are restricted to increases in canopy size and in length of internodes of *Populus* spp. after 2 years of exposure (Gielen et al., 2002). Additionally, e[CO<sub>2</sub>] increases stem diameters and number of syleptic branches in *Populus* spp., with such responses being dependent on growth period and differing among species of the same genus. Regarding *Mangifera indica* trees, the total leaf area of the crown is not affected by increasing air [CO<sub>2</sub>] (Goodfellow et al., 1997). However, increases in photosynthesis per unit leaf area mean that the photosynthetic machinery is more efficient on an area basis under e[CO<sub>2</sub>], and this would improve the overall plant photosynthesis. Finally, the rates of both fine root production and mortality, i.e. root turnover, are increased under e[CO<sub>2</sub>] (Pregitzer et al., 1995).

For simulating plant responses to e[CO<sub>2</sub>] and other climate changes, plant modelling has been used at both field (Medley et al., 2015) and ecosystem (Smith et al., 2016) scales, which are much larger scales of observation than those considering plants growing under artificial conditions. Finer scales, such as metamers, axes and plants, are usually considered in functional–structural modelling, whose paradigm considers that plants respond to their environment by adapting not only their functions but also their structures (Vos et al., 2009). Modelling of plant responses to e[CO<sub>2</sub>] rarely considers the fine metamer scale, which limits our understanding about leaf acclimation to changing environmental conditions. In fact, leaf structure may significantly affect the acclimation patterns in tree species under e[CO<sub>2</sub>] (Juurola, 2005).

As *Coffea arabica* is one of the most important crop species extensively grown in tropical conditions, it could be considered as a good model to study the impacts of e[CO<sub>2</sub>] on plant architecture and physiology. This study was focused on Arabica coffee (*Coffea arabica* L.) trees grown for 4 years inside the first FACE system in South America (Ghini et al., 2015). Recent papers on coffee plants have shown that e[CO<sub>2</sub>] might increase plant vigour (Ramalho et al., 2013; Ghini et al., 2015), and improve plant performance under warming through improvements in photosynthetic functioning (Rodrigues et al., 2016a) in protective mechanisms (Martins et al., 2016), and maintenance of mineral homeostasis (Martins et al., 2014). Our knowledge about Arabica coffee responses to e[CO<sub>2</sub>] is based on young plants inside growth chambers (Ramalho et al., 2013). The absence of water, temperature and nutritional limitations allowed enhancement of coffee photosynthesis, with almost unchanged  $g_s$  and a consequent increase in water-use efficiency under 700  $\mu\text{L CO}_2 \text{ L}^{-1}$ . After 2 years under e[CO<sub>2</sub>] in a FACE experiment, coffee plants maintained relatively high water-use efficiency and increased growth, and presented high crop yield in the first productive year (Ghini et al., 2015). The stimulation of leaf photosynthesis by e[CO<sub>2</sub>] was more prominent during the cold-dry season as compared with the rainy season. Notably, the stomatal and mesophyll conductances were also unresponsive to increasing air [CO<sub>2</sub>], as well as leaf nitrogen and phosphorus concentrations (DaMatta et al., 2016). Very

scarce information about impacts of e[CO<sub>2</sub>] on the structure of *C. arabica* is available, with young plants showing increases in height (Ghini et al., 2015).

We expected that Arabica coffee trees would respond to long-term cultivation under e[CO<sub>2</sub>] through changes in plant structure and function during the cold-dry season, when there is low sink demand. To test this hypothesis, we used functional–structural plant modelling in Arabica coffee under e[CO<sub>2</sub>] to assess changes in plant structure and photosynthesis and their relevance for overall photoassimilate production. This study is a step forward in the understanding of specific coffee plant responses to predicted e[CO<sub>2</sub>] during this century.

## MATERIALS AND METHODS

### Local and field descriptions

The experiment was carried out under the first FACE facility in South America, located at Embrapa Environment, in Jaguariúna SP, Brazil (22°43'S, 47°01'W, 570 m altitude), as previously described (Ghini et al., 2015). The soil at the experimental area is an alic, dark red latosol. The climate is subtropical, Cwa type according to the Köppen classification, with hot rainy summers and dry winters. The FACE system was located within a 7 ha coffee (*Coffea arabica* L.) plantation. Seedlings with three to four pairs of leaves of one common cultivar, 'Catuaí Vermelho IAC 144', were transplanted to the field in March 2011, in a planting design of 3.5 m between rows and 0.6 m between plants in the row. The CO<sub>2</sub> supply to air began on 25 August 2011. Our experiment was carried out after 4 years under elevated air [CO<sub>2</sub>].

The studied plants were delimited by octagon metallic rings with 10 m diameter (Ghini et al., 2015), with each ring containing four rows and 44 plants. The direct injection of pure CO<sub>2</sub> was used in half of the available octagon rings aiming at increasing air [CO<sub>2</sub>] up to 200  $\mu\text{L CO}_2 \text{ L}^{-1}$  above the current air [CO<sub>2</sub>] (treatment named a[CO<sub>2</sub>], about 390  $\mu\text{L CO}_2 \text{ L}^{-1}$ ) during the daylight period. The CO<sub>2</sub> was emitted outside of rings from tubes installed at 0.9 and 1.4 m above the soil level, following the wind direction and minimum speed of 0.5 m s<sup>-1</sup> to permit the gas mixture inside of rings (Ghini et al., 2015). The air [CO<sub>2</sub>] was measured at the centre of the rings with installed infrared gas analysers (Vaisala, CARBOCAP® Carbon Dioxide Probe GMP343, Vantaa, Finland). A multi-weather sensor model WXT520 (Vaisala, Vantaa, Finland) was used for monitoring wind speed and direction, rainfall, atmospheric pressure, temperature and relative humidity. The temporal dynamics of air temperature, rainfall and air [CO<sub>2</sub>] inside the rings where the plants were assessed are shown in Fig. 1. The 2 month periods during and before the measurements were considered to describe the subtropical cold-dry season and daily variations in air [CO<sub>2</sub>].

The NPK fertilization was done with 1750 kg ha<sup>-1</sup> year<sup>-1</sup> (20:5:15 NPK formulation) split into three applications (600/600/550 kg ha<sup>-1</sup>) during the period of active vegetative growth (from October to March). Three leaf sprays of zinc sulphate (0.6 %) and potassium chlorite (0.5 %) were carried out between October and January, and, in addition, boric acid was applied to the coffee plantation (24 kg ha<sup>-1</sup> year<sup>-1</sup> also split into three applications).

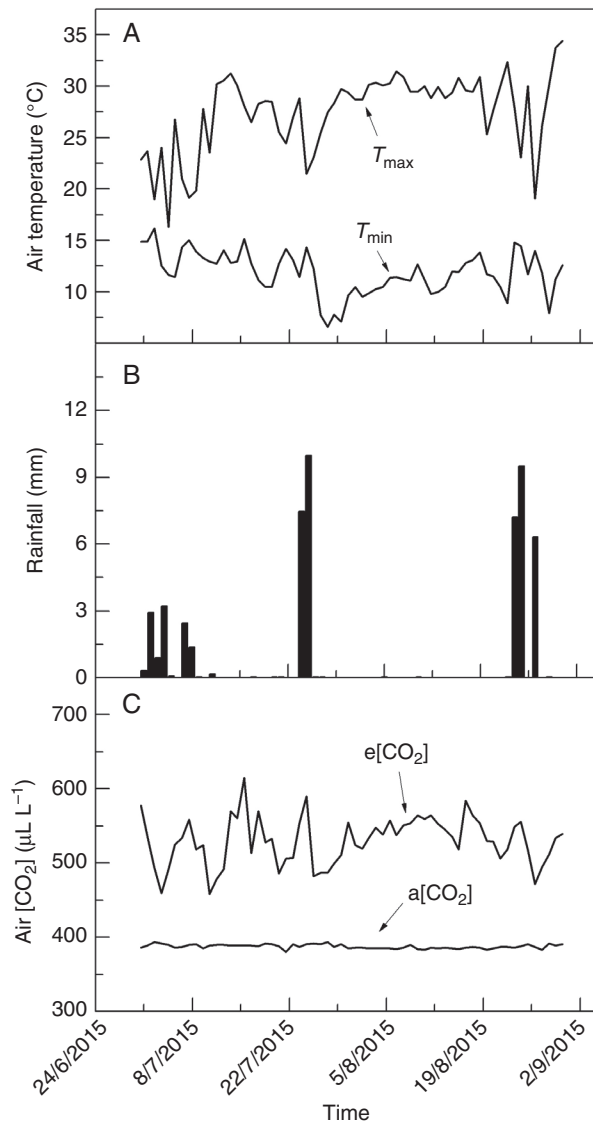


FIG. 1. Minimum and maximum daily temperatures, rainfall distribution and temporal changes in air [CO<sub>2</sub>] in elevated (e[CO<sub>2</sub>]) and actual (a[CO<sub>2</sub>]) air CO<sub>2</sub> concentration treatments registered inside the FACE octagons. Only daylight measurements were considered when the injection of CO<sub>2</sub> occurred.

#### Plant codification and software for reconstructions of mock-ups

Coffee tree architecture is described as Roux's model, characterized by a continuous growth, and dimorphic, orthotropic and plagiotropic axes (Hallé *et al.*, 1978). The orthotropic axes of the first branching order (main stems) form, at each node, two plagiotropic axes of the second order, even though sometimes no branch, or just one, develops (Matsunaga *et al.*, 2016). The orthotropic axes follow an opposite–decussate phyllotaxy. In *C. arabica*, the branching process develops plagiotropic axes from the second to the fifth orders (Supplementary Data Fig. S1). The plagiotropic axes follow an orthogonal–decussate pattern, but both internode torsion and petiole angle reorient leaves, resulting in apparent dorsiventral phyllotaxy (Dengler, 1999).

Following VPlants methodology, the coffee plant topology was decomposed into three scales (Rakocevic and

Androcioli-Filho, 2010), the plant scale, the axes scale and the metamer scale (Supplementary Data Fig. S1). The coding of coffee plants was performed in multiscale tree graphs (MTGs; Godin and Caraglio, 1998), always from the bottom to the top of the plant and axes. Coding was done during July 2015, when vegetative growth was reduced. In South-east Brazil, most of the vegetative growth of adult Arabica coffee plants occurs in the warm and rainy season (from October to March), with reduced growth occurring during the cold-dry season (from April to September; Silva *et al.*, 2004).

The coffee plants were coded according to the VPlants methodology (Pradal *et al.*, 2008). The data collection focused on eight plants for each environment (e[CO<sub>2</sub>] and a[CO<sub>2</sub>]) by methodology specified for this species (Matsunaga *et al.*, 2016). The orthotropic axis was described at the metamer scale with the following attributes: bottom and top diameter, length of each internode, leaf properties (length, width, elevation angle and cardinal orientation), position, orientation, apex mortality and total length of living parts of all second-order axes carried by the orthotropic stem. Four second-order plagiotropic axes were tagged, one for each cardinal point, to represent each layer (50 cm) of the vertical plant profile (L1, 0–50 cm; L2, 50–100 cm; L3, >100 cm). These tagged plagiotropic axes were decomposed and described at the metamer scale, as done in the orthotropic axis. In addition, the detailed description of their corresponding third- to fifth-order lateral plagiotropic branches was performed. All other second-order plagiotropic axes were described by their position at orthotropic axes, their orientation, elevation angle, and total alive branch length and terminal apex mortality.

To reconstruct the partially codified plants at the metamer scale, we used the CoffePlant3D software, which is dedicated to 3-D coffee reconstructions, integrates three interconnected modules (AmostraCafe3D, VirtualCafe3D and Cafe3D) and processes them (Matsunaga *et al.*, 2016). The final outputs of CoffePlant3D software are the MTGs, allowing 3-D reconstructions of coffee plants at the metamer scale. The leaf object for mock-ups was constructed from 16 triangles under geometry options of VPlants (Pradal *et al.*, 2008) and could accept the measured leaf attributes (leaf length, width, elevation angle and cardinal orientation) included in MTGs. Those measurements lead to accurate values of reconstructed leaf area in coffee plants (Matsunaga *et al.*, 2016), as well as estimations of leaf/plant photosynthesis. Data extraction from the MTGs was performed using AMAPstudio – Xplo software (Griffon and Coligny, 2014) to analyse the number of living and dead apexes and metamers, branching number, bottom and top axis diameters, axes length and average internode length.

#### Measurements of leaf gas exchange and light incidence inside the canopy

Leaf CO<sub>2</sub> assimilation ( $A_n$ ), stomatal conductance ( $g_s$ ), transpiration ( $E$ ) and intercellular CO<sub>2</sub> concentration ( $C_i$ ) were evaluated with a portable infrared gas analyser (Li-6400, LI-COR, Lincoln, NE, USA). Considering canopy structure, two representative plants at the centre of rings in e[CO<sub>2</sub>] and two in a[CO<sub>2</sub>] rings were chosen, and leaves of second- and third-order axes in three plant layers and four cardinal orientations were tagged for

measurements. Such a scheme of measurements allowed 10–17 gas response curves to light, for each treatment.

Measurements were taken between 09.00 and 15.00 h, on 30 and 31 July 2015 (cold-dry season). The responses of  $A_n$ ,  $g_s$  and  $E$  to photosynthetically active radiation (PAR) were determined by varying PAR in the following way: 1200, 900, 600, 300, 100, 50 and 0  $\mu\text{mol photons m}^{-2} \text{s}^{-1}$ . The highest PAR was 1200  $\mu\text{mol photons m}^{-2} \text{s}^{-1}$  as intensities of about 1000  $\mu\text{mol photons m}^{-2} \text{s}^{-1}$  are sufficiently high to saturate the photosynthetic machinery without causing photoinhibition in *C. arabica* (Cavatte *et al.*, 2012). Measurements were taken after 3–5 min at each PAR level, which was enough to reach stability in leaf gas exchange. Air temperature during the measurements was  $32.1 \pm 0.4$  °C and the leaf to air vapour pressure difference was  $3.3 \pm 1.1$  kPa.

We used the exponential model to fit the response of  $A_n$  to PAR [Eqn (1)], as done by Prado and Moraes (1997):

$$A_n = A_{\max} \left[ 1 - e^{-k(\text{PAR} - \Gamma)} \right] \quad (1)$$

where  $A_n$  is the actual photosynthesis,  $A_{\max}$  represents the maximum photosynthesis ( $\mu\text{mol CO}_2 \text{ m}^{-2} \text{s}^{-1}$ ),  $k$  is a dimensionless fitting factor and  $\Gamma$  is the light compensation point ( $\mu\text{mol photons m}^{-2} \text{s}^{-1}$ ).

The dark respiration ( $R_d$ ) was evaluated when PAR was 0  $\mu\text{mol photons m}^{-2} \text{s}^{-1}$ . The apparent quantum efficiency ( $\alpha$ ,  $\mu\text{mol CO}_2 \mu\text{mol}^{-1} \text{ photons}$ ) was calculated as the slope of the linear fit of the initial phase of the curve (until 100  $\mu\text{mol photons m}^{-2} \text{s}^{-1}$ ). The instantaneous carboxylation efficiency (CE) was estimated as  $A_n/C_i$  (Konrad *et al.*, 2005), whereas the intrinsic water-use efficiency (WUE<sub>i</sub>) was calculated as  $A_n/g_s$  (Battipaglia *et al.*, 2013).

In parallel with gas exchange measurements, PAR at leaf level was measured between 09.00 and 15.00 h in the same four representative plants in which light response curves were evaluated. A 1 m linear sensor (Li-191R Line Quantum Sensor, LI-COR) connected to a data-logger Li-1400 (LI-COR) was used to perform instantaneous measurements of PAR repeated four times in each canopy layer of each plant at intervals of 1 h (between 09.00 and 15.00 h). Two measurements were taken close to the orthotropic axis, and two others close to the outer tops of second-order axes, alternating cardinal directions N–S with E–W. We then determined the mean PAR intensities reaching the interior of the coffee canopy, which allowed us to estimate the diurnal course of photosynthesis in each layer by using the light response curves.

#### Estimations of photosynthesis and leaf area

The estimation of the leaf area (LA) per layer and CO<sub>2</sub> assimilation of the entire plant ( $A_p$ ) was performed using the software VegeSTAR (Adam *et al.*, 2006). This software simulates the spatial distribution of PAR and leaf CO<sub>2</sub> assimilation within virtual plants, and estimates LA, light interception and CO<sub>2</sub> assimilation at the plant, layer or leaf scale. The estimation of LA per coffee plant layers was allowed by attribution of Red–Green–Blue identification to each geometrical object in each 50 cm thick layer ( $z$ -axis), in input files.

The estimation of leaf photosynthesis under VegeSTAR software was based on Farquhar's model (Farquhar *et al.*, 1980) and integrated on the plant scale. Light interception and photosynthesis computing with the VegeSTAR requires information about the environment (azimuth and height of the Sun, global radiation, diffuse radiation, air temperature and air [CO<sub>2</sub>]). We considered 30 min sequenced intervals (from 09.00 to 15.00 h) of daily variation in physical and meteorological parameters during one specific day, 31 July 2015. The required parameters of the solar tracking were computed by VegeSTAR software for the co-ordinates of Jaguariúna SP, Brazil. The other necessary environmental inputs were obtained from the FACE meteorological station.

The maximum rate of ribulose-1,5-bisphosphate carboxylase/oxygenase (RuBisCO) activity ( $V_{\text{cmax}}$ ), the maximum electron transport rate ( $J_{\text{max}}$ ) driving ribulose-1,5-bisphosphate (RuBP) regeneration and  $R_d$  were also necessary for the estimation of photosynthesis at leaf and plant scales under VegeSTAR. For those estimations,  $R_d$  values were calculated from our experimental data. As response curves of  $A_n$  to increasing [CO<sub>2</sub>] were not evaluated, we used values of  $V_{\text{cmax}}$  and  $J_{\text{max}}$  estimated in coffee plants (Araújo *et al.*, 2008), considering the effects of self-shading (Rodríguez-López, 2012). This assumption was based on the absence of downregulation of photosynthesis under elevated CO<sub>2</sub> and FACE conditions (Ramalho *et al.*, 2013; Ghini *et al.*, 2015). The values of  $R_d$ ,  $V_{\text{cmax}}$  and  $J_{\text{max}}$  were attributed to each triangle that formed coffee leaf objects in input files, and varied according to air [CO<sub>2</sub>] treatment and plant layer.

The validation of estimated  $A_n$  ( $A_n'$ ) compared with measured  $A_n$  was used as a basis for further plant-scale estimations of CO<sub>2</sub> assimilation. The measured leaves were identified in VegeSTAR outputs and then photosynthesis was integrated between 09.00 and 15.00 h. Those outputs contained the computed LA and its relative  $A_n'$  of each of 16 triangles of each leaf comprising the plant foliage. Mean  $A_n'$  for 16 triangles comprising a virtual leaf was used for comparison with measured  $A_n$ . Once  $A_n'$  was validated by measured values over canopy layers,  $A_p$  was calculated considering LA of each leaf triangle (in m<sup>2</sup>) and its  $A_n'$  in the entire plant canopy.

#### Soil carbon content

Soil samples were collected in both air [CO<sub>2</sub>] treatments in July 2015. The sampling with stainless steel rings (4.8 × 3.0 cm and 55 cm<sup>3</sup>) was done at seven soil depths (0–0.05, 0.05–0.10, 0.10–0.20, 0.20–0.30, 0.30–0.40, 0.40–0.50 and 0.50–0.60 m), 0.3 m to one side of coffee lines. Total carbon concentration was determined on a CN elemental analyser TruSpec CN LECO® (Leco, St Joseph, MI, USA) (ASTM, 2000).

#### Statistical analyses

Statistical analyses and box-plot charts were performed using the R software (R Core Team, 2017). Analysis of variance (ANOVA) was used to estimate the effect of elevated [CO<sub>2</sub>] in light response curves for each of the 50 cm thick layers ( $n = 10$ –17). Mean values were compared by the Student *t*-test ( $P < 0.01$ ). The characteristics of whole-plant photosynthesis,

LA and first-order axes were analysed by one-way ANOVA ( $n = 8$ ). To analyse the structural responses to changes in [CO<sub>2</sub>] over the vertical plant profile (layers), the mixed model fitted by the 'lme' function was applied, considering plant and/or axis repetitions as fixed effects (with  $n = 25-857$ , depending on axes order). The probability level at 0.10 ( $P < 0.10$ ) was considered significant, because of large variability of responses. Only measured values of all structure parameters were analysed. The root mean square error (RMSE),  $R^2$  and bias were used to test the accuracy of leaf  $A_n'$  estimations under VegeSTAR. The RMSE was calculated in R software (R Core Team, 2017), while that of  $R^2$  and bias were computed in Excel.

## RESULTS

### Plant architecture: scale of axes

The initial assumption was that an increase in air [CO<sub>2</sub>] could have an influence on the architecture of the coffee plants. Therefore, we evaluated the attributes of axes at the metamer scale. Statistical analysis of the orthotropic axis was performed with a 90 % level of confidence due to the high variability that exists between plants grown under a[CO<sub>2</sub>] and e[CO<sub>2</sub>]. Plants under e[CO<sub>2</sub>] showed a smaller main axis (about 10 cm) and reduced average length of metamers (about 0.15 cm) as compared with those ones under a[CO<sub>2</sub>] (Table 1). Conversely, there was no difference between air [CO<sub>2</sub>] treatments in the bottom and top diameters of the first-order axes, or in the number of first-order metamers and the number of second-order branches on the main axis (Table 1).

No differences due to e[CO<sub>2</sub>] were noticed for the number of the second-order metamers (Table 2). While the longest second-order internodes were observed in the most shaded layer (L1) in both air [CO<sub>2</sub>] treatments, the shortest second-order internodes were found in L2 of plants grown under e[CO<sub>2</sub>] (Table 2). The highest average second-order length was found in L2, whereas the lowest length was noticed in the upper layer (L3), with no impact of air [CO<sub>2</sub>] treatments (Table 2). Under e[CO<sub>2</sub>], the bottom and top diameters of the second-order axes were smaller than under a[CO<sub>2</sub>]. Diameters of the second-order axes were gradually thinner from the bottom (L1) to the upper layer (L3), regardless of air [CO<sub>2</sub>].

TABLE 1. Mean  $\pm$  s.e. and ANOVA P-values ( $n = 8$ ) of the architectural characteristics of the first-order axes of coffee plants grown under elevated (e[CO<sub>2</sub>]) and actual (a[CO<sub>2</sub>]) air CO<sub>2</sub> concentration

Variables	Treatments		Effects
	e[CO <sub>2</sub> ]	a[CO <sub>2</sub> ]	P-value
Metamer number (unit)	66.8 $\pm$ 1.7	66.1 $\pm$ 1.9	0.8006
Height (cm)	154.8 $\pm$ 3.1	163.3 $\pm$ 4.6	<b>0.0702</b>
Internode length (cm)	2.3 $\pm$ 0.1	2.5 $\pm$ 0.1	<b>0.0931</b>
Bottom diameter (cm)	4.9 $\pm$ 0.2	4.8 $\pm$ 0.2	0.8830
Top diameter (cm)	0.3 $\pm$ 0.0	0.3 $\pm$ 0.0	0.3468
Branching in second-order axes (unit)	107.0 $\pm$ 3.8	104.8 $\pm$ 4.9	0.6687

P-values <0.10 were considered significant and are highlighted in bold.

As expected, the metamer number and length of the third-order axes diminished from the bottom to the top of all coffee plants (Table 2). In L1 and L2 layers, the third-order axes had fewer metamers under e[CO<sub>2</sub>] as compared with a[CO<sub>2</sub>]. The youngest third-order axis in L3 had more metamers under e[CO<sub>2</sub>] than under a[CO<sub>2</sub>]. The length of axes showed a similar trend to the metamer number in the third-order axes. The longest third-order internodes were observed in the most shaded layer (L1) in both [CO<sub>2</sub>] environments, as found for the second-order axes (Table 2). The bottom and top diameters of third-order axes were affected by air [CO<sub>2</sub>] and differed among layers (Table 2). The bottom and top diameters of third-order axes under e[CO<sub>2</sub>] were thinner than under a[CO<sub>2</sub>] in L1 and L2, opposite to that on the upper layer (L3).

The fourth-order axes were found only in L1 and L2, with shorter axes in L2 compared with L1 (Table 2). The average metamer number, length of axes and bottom diameters of the fourth-order axes were higher under a[CO<sub>2</sub>] than under e[CO<sub>2</sub>]. Like the fourth-order axes, the fifth-order axes were found only in L1 and L2 (Table 2). The metamer number, the average length of axes and the internode length of the fifth-order axes were higher in L1 under a[CO<sub>2</sub>] than under e[CO<sub>2</sub>], while the opposite was found in L2 (Table 2).

### Plant architecture: plant scale

The number of living apexes per plant layer, the dead:living apex ratio and the branching number of any axes order did not differ between air [CO<sub>2</sub>] treatments (Table 3). Only the number of metamers of the fourth- and fifth-order axes was slightly impacted by air [CO<sub>2</sub>]. In L1, the total metamer number of the fourth- and fifth-order axes of plants grown under e[CO<sub>2</sub>] diminished compared with a[CO<sub>2</sub>]. Such a structural change due to e[CO<sub>2</sub>] was inverted in L2 (Table 3).

The total average number of living apexes, total average number of living metamers per layer, mortality of apexes and average branching of axes varied significantly over the vertical profile (Table 3). The lowest number of living apexes and metamers of the second-order axes were found in L1, probably associated with the highest apex mortality occurring in this layer (about 5-fold more dead apexes than living ones). The living apex number increased gradually from L1 to L3, and the highest number of metamers of the second order was found in L2 (Table 3). The imbalance between apex number and metamer number in L3 was a consequence of the lower metamer number constructing the new second-order axes. The branching of second-order axes was similar in L1 and L2 and much lower in L3.

The third-order apexes and metamers were generally the most numerous among the axes orders at the plant scale, mainly in L2 (Table 3). The dead:living apex ratio and the branching of third-order axes were higher in L1 than in L2. The fourth-order axes had an important participation in construction of coffee trees, judging by the living apex number. Those axes had fewer metamers than the third- and second-order axes, and lower mortality than the second-order axes. The fifth-order axes were rare, constructed by low metamer number, and did not show any apex mortality at the time of evaluation. This description of coffee tree architecture is reported for the first time in this degree of detail, considering higher order axes (more than second order).

TABLE 2. Mean ± standard error (s.e.) and ANOVA P-values for the effects of CO<sub>2</sub> environment and axis position over the vertical profile on the structural characteristics of the 2<sup>nd</sup> to 5<sup>th</sup> order axes of coffee plants grown under elevated (e[CO<sub>2</sub>]) and actual (a[CO<sub>2</sub>]) air [CO<sub>2</sub>]. Four axes per each layer (L1 = 0–50 cm; L2 = 50–100 cm; L3 > 100 cm) on each plant were decomposed

Orders/Variables	Treatments/Layers						Effects		
	e[CO <sub>2</sub> ]			a[CO <sub>2</sub> ]			[CO <sub>2</sub> ]	Layer	[CO <sub>2</sub> ] × Layer
	L1	L2	L3	L1	L2	L3			
	Mean ± s.e.						P-value		
(A) Decomposed 2 <sup>nd</sup> order axes									
Metamer number (unit)	25.9 ± 2.3	31.8 ± 1.3	22.4 ± 0.7	25.0 ± 2.2	30.9 ± 1.3	22.2 ± 0.8	0.4218	0.2763	0.6852
Internode length (cm)	2.5 ± 0.1	2.1 ± 0.0	2.3 ± 0.0	2.4 ± 0.1	2.3 ± 0.0	2.3 ± 0.0	0.2403	<b>0.0022</b>	<b>0.0618</b>
(B) All 2 <sup>nd</sup> order axes									
Axis length (cm)	48.9 ± 2.1	54.7 ± 1.1	33.4 ± 0.9	48.2 ± 2.3	56.4 ± 1.3	35.1 ± 1.0	0.5937	<b>&lt;0.0001</b>	0.4759
Bottom diameter (cm)	0.7 ± 0.0	0.6 ± 0.0	0.4 ± 0.0	0.8 ± 0.0	0.6 ± 0.0	0.5 ± 0.0	<b>&lt;0.0001</b>	<b>&lt;0.0001</b>	0.9168
Top diameter (cm)	0.3 ± 0.0	0.2 ± 0.0	0.2 ± 0.0	0.4 ± 0.0	0.3 ± 0.0	0.3 ± 0.1	<b>0.0037</b>	<b>&lt;0.0001</b>	0.6007
(C) Decomposed 3 <sup>rd</sup> order axes									
Metamer number (unit)	11.6 ± 0.5	9.2 ± 0.5	6.8 ± 0.6	13.2 ± 0.8	11.0 ± 0.8	4.8 ± 0.5	0.3938	<b>&lt;0.0001</b>	<b>0.0324</b>
Internode length (cm)	2.2 ± 0.0	2.0 ± 0.1	2.0 ± 0.1	2.1 ± 0.1	1.9 ± 0.1	1.8 ± 0.1	0.4450	<b>0.0166</b>	0.6289
Axis length (cm)	24.5 ± 1.0	18.3 ± 0.9	13.9 ± 1.3	27.0 ± 1.6	22.2 ± 1.7	9.8 ± 1.3	0.3529	<b>&lt;0.0001</b>	<b>0.0817</b>
Bottom diameter (cm)	0.3 ± 0.0	0.3 ± 0.0	0.3 ± 0.0	0.3 ± 0.0	0.3 ± 0.0	0.2 ± 0.0	<b>0.0326</b>	<b>&lt;0.0001</b>	<b>0.0019</b>
Top diameter (cm)	0.1 ± 0.0	0.1 ± 0.0	0.2 ± 0.0	0.2 ± 0.0	0.1 ± 0.0	0.1 ± 0.0	<b>0.0106</b>	<b>0.0703</b>	<b>0.0656</b>
(D) Decomposed 4 <sup>th</sup> order axes									
Metamer number (unit)	7.1 ± 0.4	6.8 ± 0.5	-	9.4 ± 0.7	7.0 ± 0.8	-	<b>0.0485</b>	0.1624	0.1397
Internode length (cm)	2.0 ± 0.1	1.9 ± 0.1	-	2.0 ± 0.1	2.0 ± 0.1	-	0.8201	0.5653	0.9399
Axis length (cm)	14.8 ± 1.3	13.3 ± 1.2	-	20.0 ± 1.8	15.1 ± 2.1	-	<b>0.0155</b>	<b>0.0800</b>	0.2012
Bottom diameter (cm)	0.2 ± 0.0	0.2 ± 0.0	-	0.3 ± 0.0	0.2 ± 0.0	-	<b>0.0217</b>	0.8106	0.1476
Top diameter (cm)	0.1 ± 0.0	0.1 ± 0.0	-	0.1 ± 0.0	0.2 ± 0.0	-	0.9664	0.8521	0.4102
(E) Decomposed 5 <sup>th</sup> order axes									
Metamer number (unit)	5.8 ± 0.8	6.6 ± 1.7	-	7.8 ± 2.0	2.7 ± 0.3	-	0.8401	0.3078	<b>0.0464</b>
Internode length (cm)	1.7 ± 0.2	2.4 ± 0.4	-	1.6 ± 1.0	1.0 ± 0.1	-	0.1269	0.4147	<b>0.0571</b>
Axis length (cm)	11.4 ± 2.4	18.6 ± 5.0	-	15.7 ± 5.3	2.7 ± 0.4	-	0.5898	0.9983	<b>0.0305</b>
Bottom diameter (cm)	0.2 ± 0.0	0.2 ± 0.0	-	0.2 ± 0.0	0.2 ± 0.0	-	0.7324	0.9705	0.3595
Top diameter (cm)	0.1 ± 0.0	0.1 ± 0.0	-	0.1 ± 0.0	0.1 ± 0.0	-	0.9603	0.8626	0.6788

$P < 0.10$  were considered significant and highlighted in bold.

Based on measurements and their integrations by using VPlants and CoffePlant3D software, the 3-D reconstructions were performed ( $n = 8$ ). The global plant shapes after 4 years of growth under a[CO<sub>2</sub>] and e[CO<sub>2</sub>] are shown on two plants of average LA (Fig. 2). The LA per canopy layer was computed in VegeSTAR and its average values across the tree canopy layers are also shown (Fig. 2). The results were unexpected, and we found a strong LA reduction under e[CO<sub>2</sub>], mainly at the lowest and the highest canopy layers. LA of the L1 and L3 layers was reduced by approx. 50 % under e[CO<sub>2</sub>] when compared with the corresponding layers under a[CO<sub>2</sub>].

#### Light response curves of leaf gas exchange

Light response curves revealed that leaf CO<sub>2</sub> assimilation ( $A_n$ ) was increased under e[CO<sub>2</sub>], with the highest differences between [CO<sub>2</sub>] treatments being found in L3 (Fig. 3). The maximum photosynthesis ( $A_{n,max}$ ) was higher under e[CO<sub>2</sub>] as compared with a[CO<sub>2</sub>] both in L2 ( $2.95 \pm 0.41$  vs.  $1.63 \pm 0.24 \mu\text{mol m}^{-2} \text{s}^{-1}$ ) and in L3 ( $4.33 \pm 0.69$  vs.  $1.13 \pm 0.14 \mu\text{mol m}^{-2} \text{s}^{-1}$ ) layers (Fig. 3A–C), showing the usual low values for this species in the cold-dry season. The light compensation point ( $I$ ) was reduced by e[CO<sub>2</sub>] in L2

( $31 \pm 3$  vs.  $50 \pm 9 \mu\text{mol m}^{-2} \text{s}^{-1}$  under a[CO<sub>2</sub>]) and L3 ( $29 \pm 4$  vs.  $74 \pm 11 \mu\text{mol m}^{-2} \text{s}^{-1}$  under a[CO<sub>2</sub>]) layers. The apparent quantum efficiency ( $\alpha$ ) in L1 and L3 layers of field-grown coffee plants was improved under e[CO<sub>2</sub>], as shown in Fig. 3A and C. Non-significant changes ( $P = 0.1577$ ) induced by e[CO<sub>2</sub>] were found in dark respiration ( $R_d$ ) of field-grown coffee trees, with values varying between  $1.04 \pm 0.15$  and  $1.61 \pm 0.16 \mu\text{mol m}^{-2} \text{s}^{-1}$  through the canopy layers and [CO<sub>2</sub>] treatments.

Regardless of light intensity,  $g_s$  was always higher under e[CO<sub>2</sub>], and differences between [CO<sub>2</sub>] treatments decreased from L3 to L1 (Fig. 3D–F). As a consequence, leaf transpiration rates in L2 and L3 were increased by high air [CO<sub>2</sub>] (Supplementary Data Fig. S2). The instantaneous carboxylation efficiency (CE) was higher under e[CO<sub>2</sub>] in L3 and such an effect of e[CO<sub>2</sub>] was inverted in L1 (Fig. 4A, C). Non-significant changes in CE were found in L2. The intrinsic water-use efficiency ( $WUE_i$ ) followed the same pattern of CE, with e[CO<sub>2</sub>] causing higher  $WUE_i$  in L3 and lower  $WUE_i$  in L1 as compared with a[CO<sub>2</sub>] (Fig. 4D–F).

$A_n$  was well-correlated to CE through the canopy profile but air [CO<sub>2</sub>] had a significant influence on this correlation (Fig. 5A). In general, the slope of  $A_n \times CE$  was 1.6 times higher under e[CO<sub>2</sub>], indicating that  $A_n$  is more responsive to increases of CE under e[CO<sub>2</sub>].  $A_n$  was also well correlated to  $g_s$  (Fig. 5B), but such a correlation was dependent on the canopy layer and air

TABLE 3. Mean  $\pm$  s.e. and ANOVA P-values for the effects of [CO<sub>2</sub>] treatment {elevated (e[CO<sub>2</sub>]) and actual (a[CO<sub>2</sub>]) air CO<sub>2</sub> concentration} and axis position over the vertical profile (L1 = 0–50 cm; L2 = 50–100 cm; L3 > 100 cm) on the number of apices, living metamers, dead meristems per living meristems and branches of the second- to fifth-order axes of coffee plants

Axis order/layers	Treatments		ANOVA effects (P-value)			Treatments		ANOVA effects (P-value)			
	e[CO <sub>2</sub> ]	a[CO <sub>2</sub> ]	[CO <sub>2</sub> ]	Layer	[CO <sub>2</sub> ] × layer	e[CO <sub>2</sub> ]	a[CO <sub>2</sub> ]	[CO <sub>2</sub> ]	Layer	[CO <sub>2</sub> ] × layer	
	Mean $\pm$ s.e.					Mean $\pm$ s.e.					
Living apices						Living metamers					
Second	1	5.0 $\pm$ 0.8	4.8 $\pm$ 1.2	0.6743	<b>&lt;0.0001</b>	0.6844	368.6 $\pm$ 35.0	337.4 $\pm$ 51.2	0.6794	<b>0.0946</b>	0.6547
	2	24.6 $\pm$ 1.7	24.6 $\pm$ 2.4				843.9 $\pm$ 90.2	918.1 $\pm$ 60.0			
	3	37.8 $\pm$ 3.5	35.6 $\pm$ 3.4				493.6 $\pm$ 74.0	551.5 $\pm$ 78.5			
Third	1	64.8 $\pm$ 7.4	68.3 $\pm$ 8.9	0.4767	<b>0.0147</b>	0.9332	620.9 $\pm$ 65.9	567.8 $\pm$ 89.2	0.5334	<b>0.0002</b>	0.8203
	2	117.4 $\pm$ 7.4	140.0 $\pm$ 20.6				972.8 $\pm$ 115.9	840.0 $\pm$ 89.7			
	3	15.8 $\pm$ 3.5	22.4 $\pm$ 4.1				102.6 $\pm$ 16.9	104.3 $\pm$ 22.9			
Fourth	1	24.1 $\pm$ 3.9	29.6 $\pm$ 5.5	0.6757	0.2850	0.1544	159.3 $\pm$ 27.3	220.4 $\pm$ 35.2	0.9812	<b>0.0646</b>	<b>0.0283</b>
	2	26.8 $\pm$ 4.5	18.6 $\pm$ 5.1				169.9 $\pm$ 33.9	107.5 $\pm$ 28.8			
Fifth	1	4.0 $\pm$ 0.7	6.8 $\pm$ 2.0	0.2359	<b>0.0008</b>	0.1233	24.1 $\pm$ 3.9	47.1 $\pm$ 13.9	0.2149	<b>0.0007</b>	<b>0.0521</b>
	2	1.5 $\pm$ 0.8	1.4 $\pm$ 0.7				10.9 $\pm$ 6.1	5.5 $\pm$ 2.4			
Ratio of dead:living apices						Branching number per axis					
Second	1	5.2 $\pm$ 1.3	4.6 $\pm$ 0.9	0.7579	<b>&lt;0.0001</b>	0.6461	2.9 $\pm$ 0.3	3.2 $\pm$ 0.3	0.2173	<b>&lt;0.0001</b>	0.8491
	2	0.8 $\pm$ 0.1	0.8 $\pm$ 0.2				2.9 $\pm$ 0.3	3.4 $\pm$ 0.5			
	3	0.04 $\pm$ 0.01	0.06 $\pm$ 0.03				0.39 $\pm$ 0.07	0.57 $\pm$ 0.09			
Third	1	0.1 $\pm$ 0.0	0.2 $\pm$ 0.0	0.3478	<b>&lt;0.0001</b>	0.2477	0.4 $\pm$ 0.1	0.4 $\pm$ 0.1	0.5052	<b>&lt;0.0001</b>	0.5860
	2	0.04 $\pm$ 0.01	0.04 $\pm$ 0.03				0.23 $\pm$ 0.03	0.13 $\pm$ 0.03			
Fourth	1	0.1 $\pm$ 0.1	0.4 $\pm$ 0.4	0.2881	0.1686	0.4241	0.2 $\pm$ 0.0	0.2 $\pm$ 0.1	0.3339	<b>0.0010</b>	0.7612
	2	0.02 $\pm$ 0.02	0.07 $\pm$ 0.04				0.05 $\pm$ 0.02	0.07 $\pm$ 0.03			

P-values <0.10 were considered significant and are highlighted in bold.

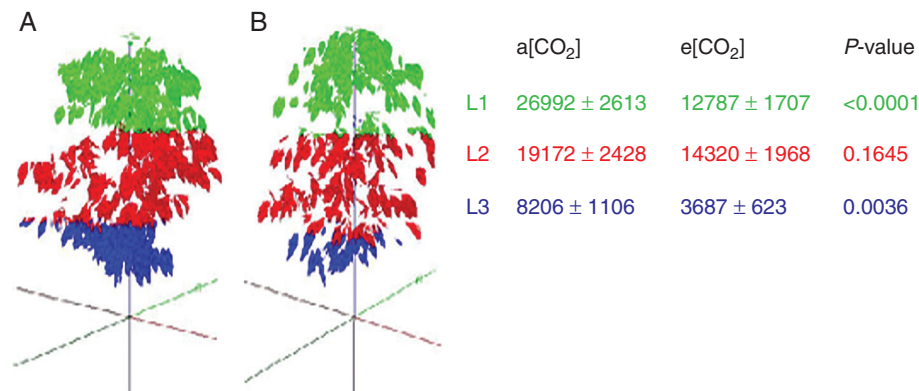


FIG. 2. Reconstructions of Arabica coffee plants cultivated under elevated (e[CO<sub>2</sub>], in A) and actual (a[CO<sub>2</sub>], in B) air [CO<sub>2</sub>] environments and mean ( $n = 8$ ,  $\pm$  s.e.) leaf area (cm<sup>2</sup>), reconstructed for the fourth cold-dry season (July 2015) per layer of the vertical profile of plants. ANOVA P-values are indicated. The colours separate three plant layers L1 (0–50 cm), L2 (50–100 cm) and L3 (>100 cm).

[CO<sub>2</sub>]. Under a[CO<sub>2</sub>], the correlation between  $A_n$  and  $g_s$  was significant in all canopy layers and the slopes varied between 274 (L1) and 482 (L3). When plants under e[CO<sub>2</sub>] were considered, significant correlations between  $A_n$  and  $g_s$  were found only in L2 and L3, and the slopes were 532 and 868, respectively (Fig. 5B).

light response curves of photosynthesis (Fig. 3A–C), we were able to estimate leaf CO<sub>2</sub> assimilation ( $A_n'$ ) throughout the diurnal course (Fig. 6D–F). Coffee plants under e[CO<sub>2</sub>] had higher  $A_n'$  than plants under a[CO<sub>2</sub>], regardless of canopy layer and time of day.

#### Diurnal course of leaf CO<sub>2</sub> assimilation

Due to changes in leaf area through the canopy profile, light availability in all canopy layers was higher in coffee plants under e[CO<sub>2</sub>], mainly up to 13.00 h (Fig. 6A–C). By considering the

#### Modelling leaf and plant photosynthesis

Measured photosynthetic rates ( $A_n$ ) were compared with photosynthetic rates estimated under VegeSTAR ( $A_n'$ ) (Fig. 7A).  $A_n'$  values were slightly overestimated when

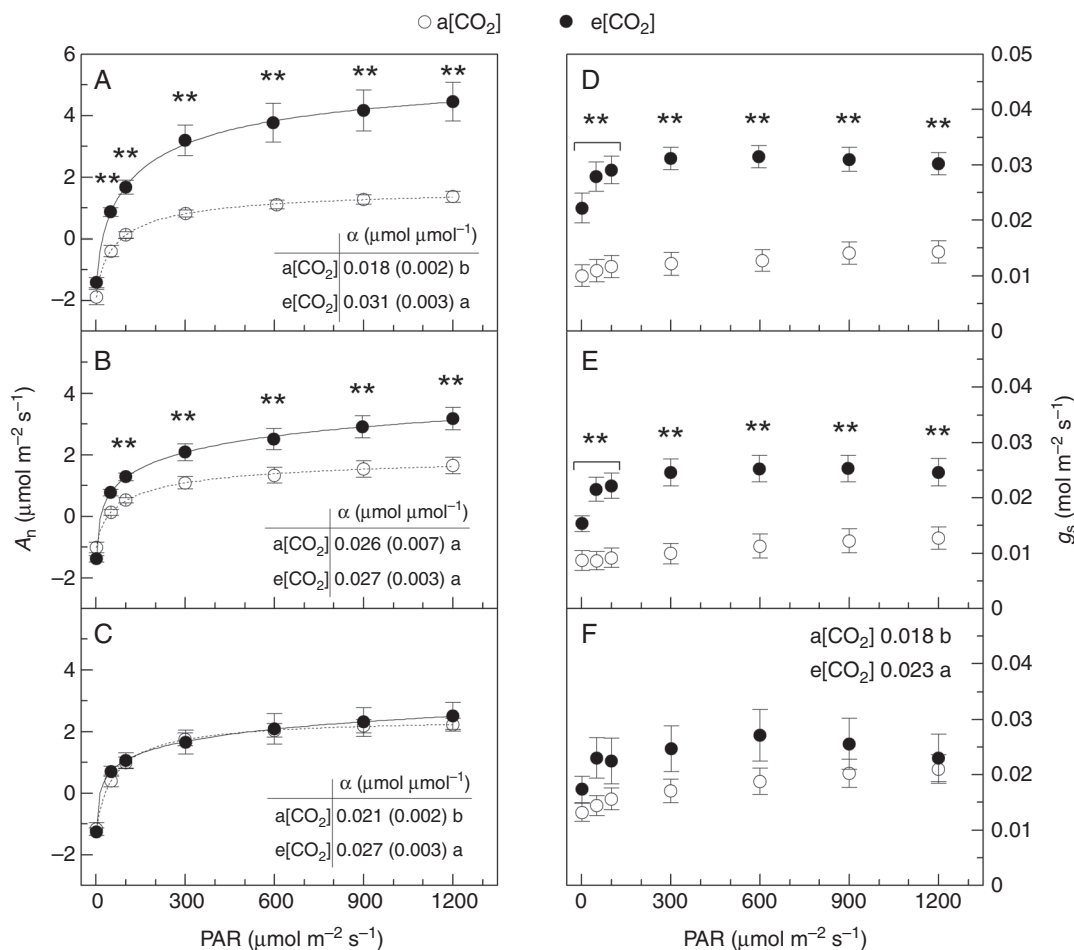


FIG. 3. Light response curves of leaf CO<sub>2</sub> assimilation ( $A_n$ , in A–C) and stomatal conductance ( $g_s$ , in D–F) in field-grown coffee trees under actual ( $a[\text{CO}_2]$ ) and elevated ( $e[\text{CO}_2]$ ) air CO<sub>2</sub> concentration. Apparent quantum efficiency ( $\alpha$ ) is shown in (A) and (C). Measurements were taken in three canopy layers: 0–50 cm (L1, in C, F); 50–100 cm (L2, in B, E); >100 cm (L3, in A, D). Each symbol is the mean value of 10–17 replications ( $\pm$  s.e.). \*\* and different letters (in F) indicate statistical difference between [CO<sub>2</sub>] treatments at  $P < 0.01$ .

compared with  $A_n$ , with a bias of 0.059. RMSE was low (0.089 on a scale of  $5.5 \mu\text{mol m}^{-2} \text{s}^{-1}$ ) and estimates were very close to the fitted regression line ( $R^2 = 0.97$ ). Well-adjusted estimations at the leaf scale (Fig. 7A) allowed the daily estimation of whole-plant photosynthesis between 09.00 and 15.00 h, when intensive CO<sub>2</sub> assimilation occurs (Fig. 7B). Due to the higher photosynthetic capacity of leaves under  $e[\text{CO}_2]$ , the impact of LA reduction (Fig. 2) was mitigated at the plant scale (Fig. 7B). The whole-plant photosynthesis estimated under  $e[\text{CO}_2]$  significantly exceeded the values attained under  $a[\text{CO}_2]$ .

#### Soil carbon

During the cold-dry season of the fourth year of coffee cultivation under the FACE facility, a higher total soil carbon concentration was found under  $e[\text{CO}_2]$  compared with  $a[\text{CO}_2]$  at all soil depths below 0.05 m (Fig. 8).

## DISCUSSION

### Architectural changes in coffee canopy under high air [CO<sub>2</sub>]: detailed analyses over the vertical plant profile

The first novelty of this work is that the analyses of coffee architecture were done over the vertical plant profile, considering all five axis orders (Tables 1–3). Coffee plants are usually compared based on the length of the second-order plagiotropic axes (Cilas *et al.*, 1998), or plant height and characters of sampled second-order axes in the middle third of plants (Ghini *et al.*, 2015; Ronchi *et al.*, 2016). In our study, detailed measurements, estimations and analyses of coffee plant architecture were conducted. The third-order axes appeared along all the plant profile (Tables 1–2), whereas the fourth- and fifth-order axes appeared in L1 and L2 in the fourth year of field cultivation. Although abscission of the fourth- and fifth-order axes is a phenological event under subtropical cold-dry seasons (Camargo and Camargo, 2001), various fourth- and fifth-order axes still were present.



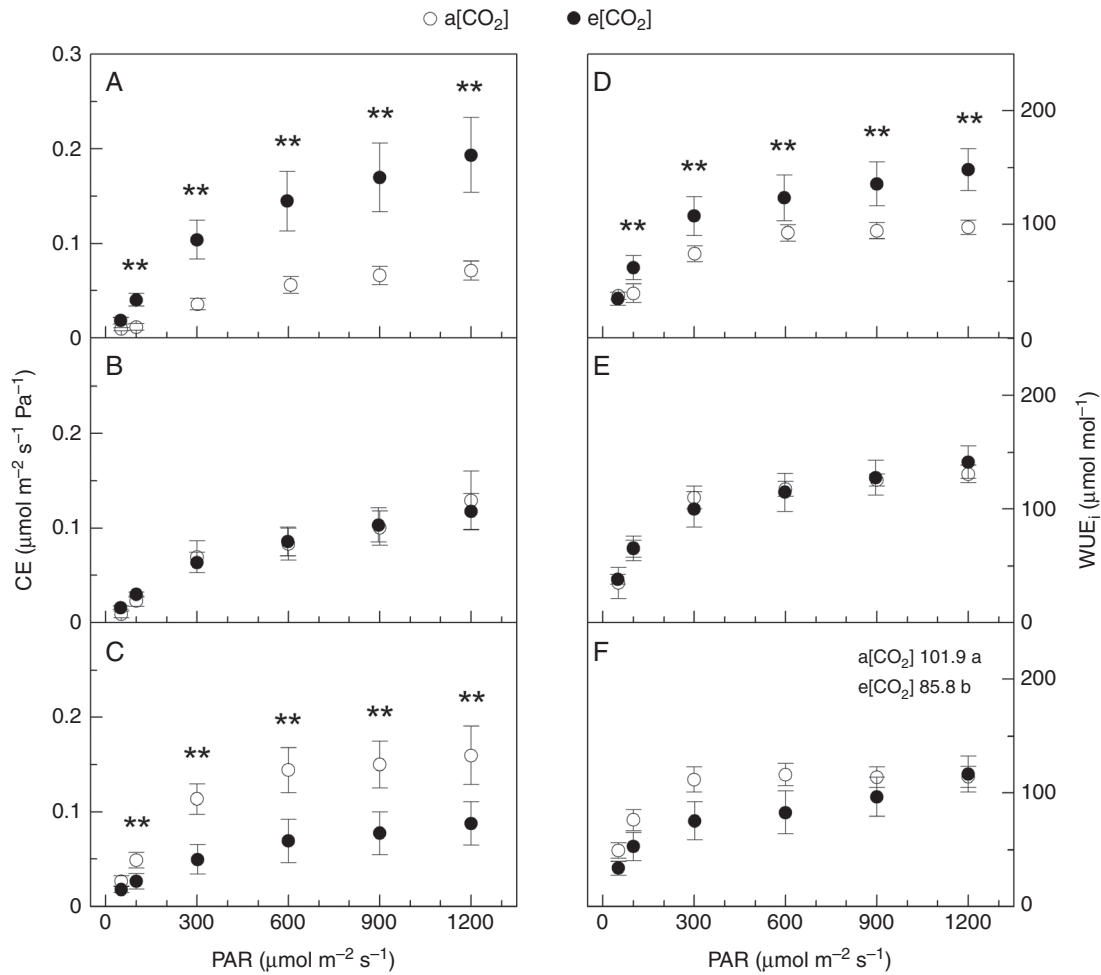


FIG. 4. Light response curves of instantaneous carboxylation efficiency (CE, in A–C) and intrinsic water-use efficiency (WUE<sub>i</sub>, in D–F) in field-grown coffee trees under actual (a[CO<sub>2</sub>]) and elevated (e[CO<sub>2</sub>]) air CO<sub>2</sub> concentration. Measurements were taken in three canopy layers: 0–50 cm (L1, in C, F); 50–100 cm (L2, in B, E); >100 cm (L3, in A, D). Each symbol is the mean value of 10–17 replications ( $\pm$  s.e.). \*\* and different letters (in F) indicate statistical difference between [CO<sub>2</sub>] treatments at  $P < 0.01$ .

Mature coffee trees grown under e[CO<sub>2</sub>] would probably invest more carbon into the newest aerial structures of third- to fifth-order axes that were exposed to full sunlight as compared with those under a[CO<sub>2</sub>], and lower second-order axes over the whole plant structure. Such an investment would promote  $A_n$  under more adequate light conditions (Fig. 3), balancing reduction in leaf area (Fig. 2) when overall photoassimilate production is taken into account.

#### Structural and functional changes induced by high air [CO<sub>2</sub>] suggest carbon partitioning to the root system

Usually, the LA of young *C. arabica* trees doubles from spring to summer under high water availability (Rodrigues *et al.*, 2016b). During the fourth cold-dry season and after long-term e[CO<sub>2</sub>] conditions, coffee trees clearly showed a reduction in LA (Fig. 2), as compared with plants under a[CO<sub>2</sub>]. This structural change was unexpected as higher leaf photosynthetic rates were found in both L2 and L3 when grown under e[CO<sub>2</sub>], regardless of the light level or time of day (Figs 3A, B and 6D–F). In fact, the overall CO<sub>2</sub> uptake by the coffee canopy was

increased under e[CO<sub>2</sub>] as compared with a[CO<sub>2</sub>] (Fig. 7B), suggesting higher plant growth and canopy size under e[CO<sub>2</sub>]. However, such a supposition was not true when considering reconstructed LA based on measurements (Matsunaga *et al.*, 2016). As the total number of living metamers did not differ between two CO<sub>2</sub> treatments (Rakocevic *et al.*, 2017), LA reduction could be a consequence of seasonal limiting conditions (low water availability) and/or higher leaf shed accumulated over the last two cold-dry seasons, which was not noticed in young coffee plants by Ghini *et al.* (2015).

An increase in  $g_s$  of coffee plants under e[CO<sub>2</sub>] was another interesting finding, as shown in Fig. 3D–F. In fact, partial stomatal closure is a general plant response to e[CO<sub>2</sub>] (Mot, 1990), and previous reports showed that coffee leaf stomata were mostly unresponsive to increasing air [CO<sub>2</sub>] (Ghini *et al.*, 2015; Rodrigues *et al.*, 2016a). Under low  $g_s$ , high air [CO<sub>2</sub>] would allow plants to maintain photosynthetic rates, as is also the case under high air temperatures (Martins *et al.*, 2016; Rodrigues *et al.*, 2016b).

In young plants of *C. arabica* grown under the FACE facility, higher  $A_n$  values under e[CO<sub>2</sub>] compared with a[CO<sub>2</sub>] were observed only during the cold-dry season (Ghini *et al.*, 2015).

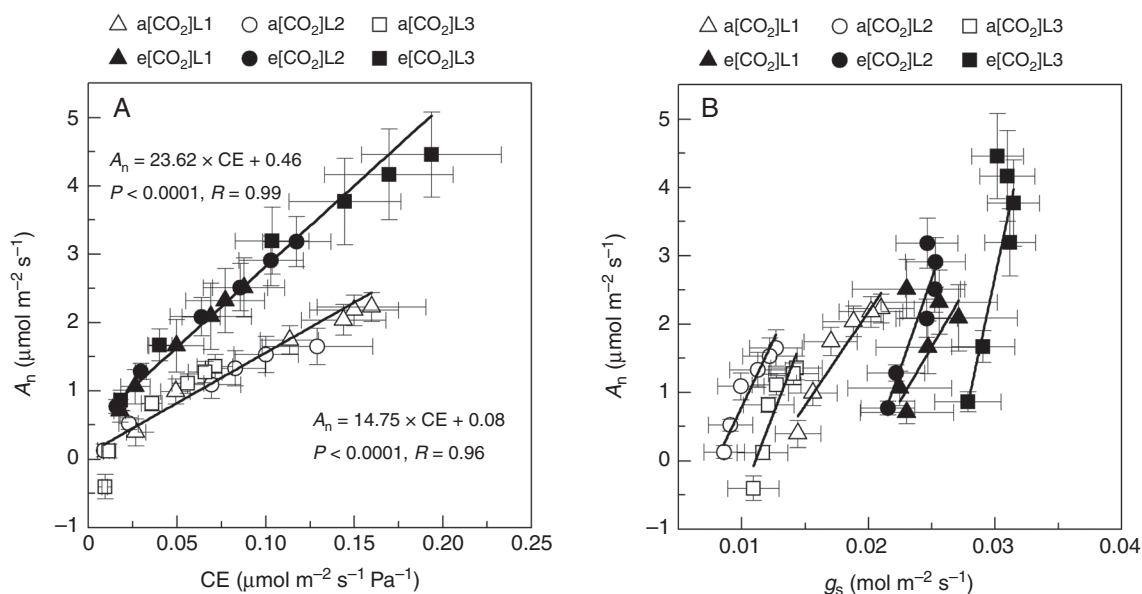


FIG. 5. Correlations between leaf CO<sub>2</sub> assimilation ( $A_n$ ) and instantaneous carboxylation efficiency (CE, in A) and between  $A_n$  and stomatal conductance ( $g_s$ , in B) in field-grown coffee trees under actual ( $a[CO_2]$ ) and elevated ( $e[CO_2]$ ) air CO<sub>2</sub> concentration. Measurements were taken in three canopy layers: 0–50 cm (triangles); 50–100 cm (circles); >100 cm (squares). Each symbol is the mean value of 10–17 replications ( $\pm$  s.e.). In (B), the correlations are represented by the following equations:  $a[CO_2] - L1, y = 274.29x - 3.31, r = 0.94, P = 0.004$ ; L2,  $y = 390.71x - 3.12, r = 0.95, P = 0.003$ ; L3,  $y = 482.30x - 5.34, r = 0.90, P = 0.014$ ;  $e[CO_2] - L1, y = 316.72x - 6.25, r = 0.62, P = 0.191$ ; L2,  $y = 532.96x - 10.65, r = 0.96, P = 0.002$ ; L3,  $y = 868.07x - 23.34, r = 0.94, P = 0.005$ .

For that reason and for evaluating long-term responses, analyses were done during the fourth cold-dry season (Fig. 1A). In this season, low air temperature and low water availability significantly reduce  $g_s$  in coffee trees (Silva *et al.*, 2004). On the other hand, it is well known that turgor is essential for stomatal opening, with coffee plants showing the highest  $g_s$  during the rainy season (Silva *et al.*, 2004). Our data thus suggest that coffee trees under  $e[CO_2]$  are less water stressed or more hydrated than plants under  $a[CO_2]$ , as the latter exhibited lower  $g_s$  and leaf CO<sub>2</sub> assimilation (Fig. 3). For increasing shoot water status and then stomatal aperture, plants should be able to explore soil resources and increase water uptake (Tron *et al.*, 2015). As coffee trees under  $e[CO_2]$  presented higher  $g_s$ , higher photosynthesis and lower canopy size than plants under  $a[CO_2]$  during the cold-dry season, photoassimilates could be driven to the root system rather than to plant shoots. This would improve water uptake and then leaf turgor, causing higher stomatal conductance (Fig. 3D–F) and transpiration (Supplementary Data Fig. S2).

Meta-analyses show that atmospheric CO<sub>2</sub> enrichment stimulates both the input and the turnover of carbon in soil (van Groenigen *et al.*, 2014), supporting our results of higher carbon content over the soil profile (Fig. 8). We argue that such an increase in soil carbon amount under  $e[CO_2]$  (Fig. 8) was not caused by decomposition of coffee residues, which is not affected by  $e[CO_2]$  (Vidal *et al.*, 2015). The slight tendency for higher investments in roots under  $e[CO_2]$  has already been reported in coffee seedlings (Batista, 2015). The turnover of fine roots has been recognized as an important source of carbon, being responsible for increasing the soil carbon concentration when tree species are grown under  $e[CO_2]$  (Iversen *et al.*, 2008). Under low water availability and  $e[CO_2]$ , various woody species tend to allocate more biomass to roots (Curtis and Wang, 1998), supporting our hypothesis about the shift

in photoassimilate partitioning to roots in coffee trees under  $e[CO_2]$  and low water availability. Such a hypothesis should be further tested in field-grown coffee trees under  $e[CO_2]$ , where root growth is not limited and resources, such as water, vary in a seasonal manner.

#### Underlying factors leading to increased photosynthesis and water-use efficiency under $e[CO_2]$

Elevated air [CO<sub>2</sub>] increased coffee photosynthesis but such an effect varied within the plant canopy (Fig. 3A–C). While leaves positioned at the bottom canopy layer (i.e. L1) did not respond to  $e[CO_2]$ , leaves of the upper layer (i.e. L3) presented a significant enhancement of photosynthesis due to  $e[CO_2]$ , regardless of the instantaneous light intensity. The oldest leaves in Arabica coffee were about 8 months old and supported by fourth- and fifth-order axes in the bottom layers (Correia *et al.*, 2017). We measured leaves on second- and third-order axes, as a preference, which excludes leaf unresponsiveness caused by ageing. Our results indicate that self-shading offsets the stimulatory effect of high air [CO<sub>2</sub>] in coffee trees. This would have an important implication for plant modelling, as 12 % of total leaf area in adult coffee trees was found at the bottom canopy position (Fig. 2). In this way, predictions about the responsiveness of coffee photosynthesis to high air [CO<sub>2</sub>] would overestimate the actual response in coffee plantations, affecting either estimations of biomass production or crop yield.

The stimulatory effect of  $e[CO_2]$  on photosynthesis in the intermediate and upper canopy layers was associated with higher  $g_s$  (Fig. 3A, B, D, E), a possible consequence of carbon partitioning to the root system as discussed previously. As stomata are less closed under  $e[CO_2]$ , one would argue that more CO<sub>2</sub> is available for photosynthesis. Regarding

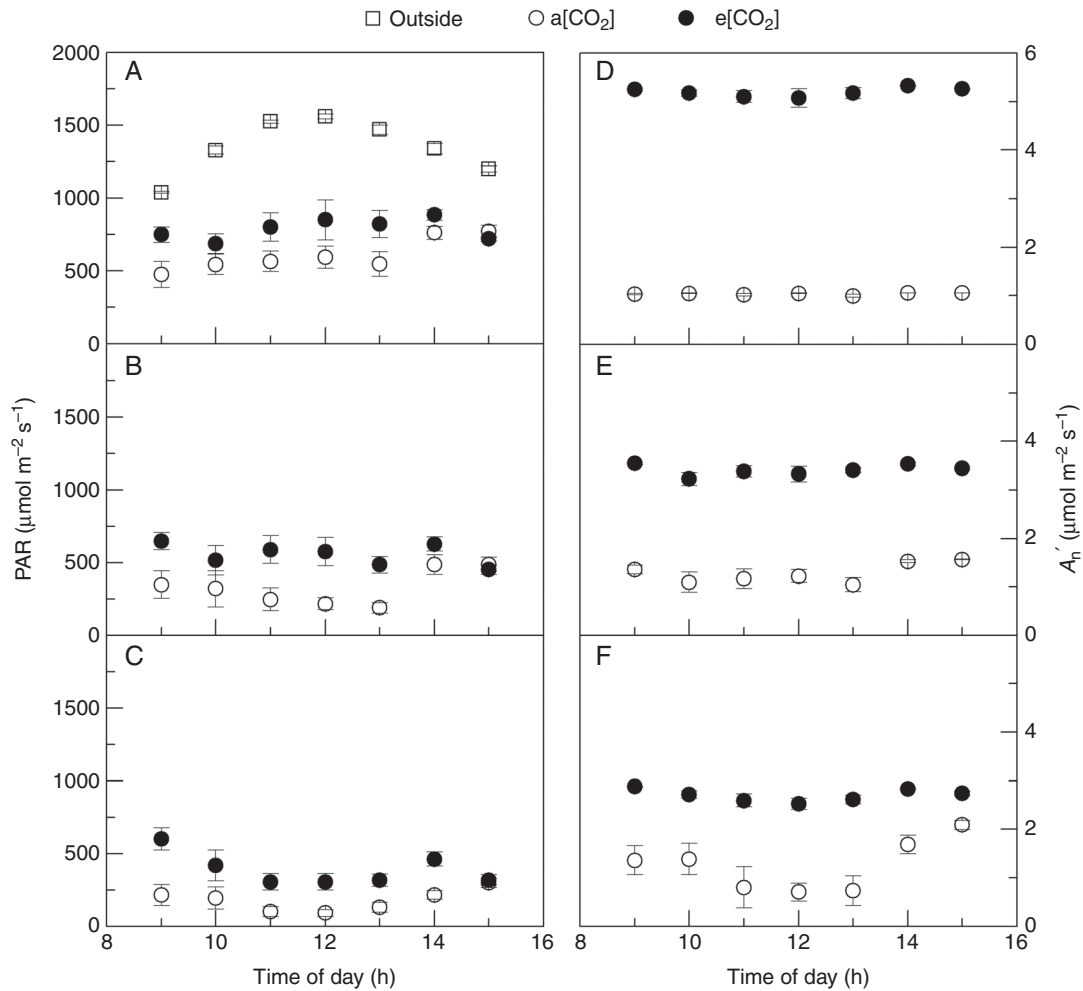


FIG. 6. Diurnal course of photosynthetic active radiation (PAR, in A–C) and estimated leaf CO<sub>2</sub> assimilation ( $A_n'$ , in D–F) in field-grown coffee trees under actual ( $a[CO_2]$ ) and elevated ( $e[CO_2]$ ) air CO<sub>2</sub> concentration. Values were estimated in three canopy layers: 0–50 cm (L1, in C, F); 50–100 cm (L2, in B, E); >100 cm (L3, in A, D). Each symbol is the mean value of eight replications ( $\pm$  s.e.). PAR measurements outside the coffee canopy are shown in (A).

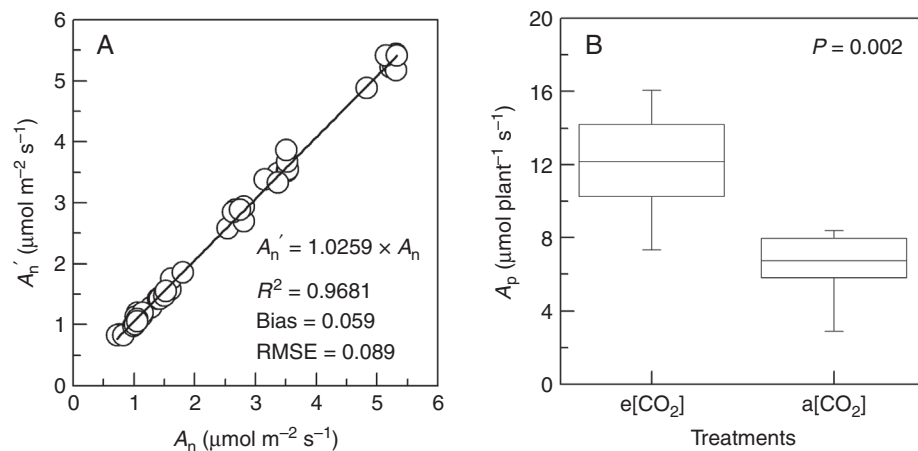


FIG. 7. Comparison between estimated ( $A_n'$ ) and measured ( $A_n$ ) leaf net photosynthesis (in A) and whole-plant photosynthesis ( $A_p$ , in B) of Arabica coffee computed under VegeSTAR from mock-ups produced in VPlants, integrating the hours of the most intensive daily assimilation. In (A), the root mean square error (RMSE), the  $R^2$ , the bias and the 1:1 line are indicated. In (B), minimum, first quartile, median, third quartile and maximum values of  $A_p$ , and the  $P$ -value of ANOVA ( $n = 8$ ) are shown. Plants were cultivated under elevated ( $e[CO_2]$ ) and actual ( $a[CO_2]$ ) air CO<sub>2</sub> concentration environments. Estimations were done for the fourth cold-dry season (31 July 2015).

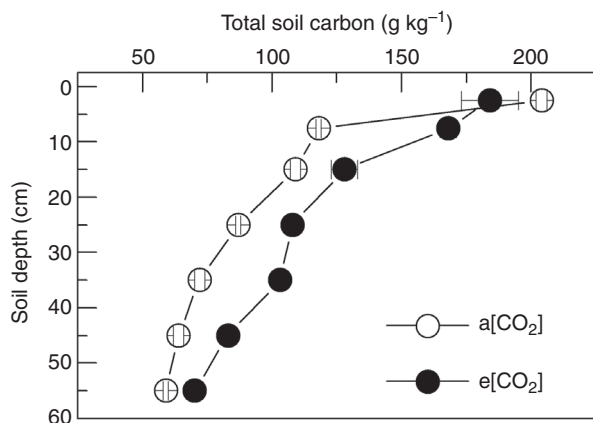


FIG. 8. Profile of total carbon concentration in soil under actual ( $a[\text{CO}_2]$ ) and elevated ( $e[\text{CO}_2]$ ) air  $\text{CO}_2$  concentration. Each symbol is the mean value of three replications ( $\pm$  s.e.).

photochemical reactions, parallel increases in the apparent quantum efficiency and photosynthesis due to  $e[\text{CO}_2]$  were found only at L3 (Fig. 3A). This finding indicates that improved photochemistry is associated with increasing coffee photosynthesis under high air  $[\text{CO}_2]$  only at canopy positions exposed to high light (Fig. 6A). Accordingly, coffee leaves presented a large increase in the instantaneous carboxylation efficiency when exposed to  $e[\text{CO}_2]$  and positioned at the upper canopy layer (Fig. 4A). Such improvements in photosynthetic machinery are supported by previous studies showing higher  $A_n$ ,  $J_{\text{max}}$  and  $V_{\text{cmax}}$  (Ramalho *et al.*, 2013; Rodrigues *et al.*, 2016) and lower photoinhibition (Martins *et al.*, 2016) in plants under  $e[\text{CO}_2]$ . As already known, high air  $[\text{CO}_2]$  increases the ratio between  $[\text{CO}_2]$  and  $[\text{O}_2]$ , inhibiting the oxygenase activity of RuBisCO, and then reducing the photorespiration rate (Drake *et al.*, 1997). This phenomenon is accompanied by increases in  $\text{CO}_2$  fixation through the carboxylase activity in  $\text{C}_3$  species (Carmo-Silva *et al.*, 2015), explaining the higher CE of coffee trees under  $e[\text{CO}_2]$  (Fig. 4A). Taking those results together, our data suggest that high air  $[\text{CO}_2]$  improved coffee photosynthesis through increases in  $g_s$  (L2 and L3), and stimulation of photochemical (L3) and biochemical (L3) reactions under limiting water supply.

When comparing the correlation between  $A_n$  and CE (Fig. 5A), we found higher photosynthesis under  $e[\text{CO}_2]$  than under  $a[\text{CO}_2]$  for a given instantaneous carboxylation rate. This indicates that factors other than CE are causing higher photosynthesis under  $e[\text{CO}_2]$ . We also found higher responsiveness of  $A_n$  to CE (given by the slopes) under  $e[\text{CO}_2]$  (Fig. 5A), indicating that a unit change in CE causes larger changes in  $A_n$  under  $e[\text{CO}_2]$  than under  $a[\text{CO}_2]$ . This supports the higher investment of resources in the photosynthetic machinery of coffee trees under  $e[\text{CO}_2]$ . For instance, increased investment of nitrogen in sun leaves enhanced light-saturated photosynthesis under  $e[\text{CO}_2]$  (Herrick and Thomas, 1999).

Correlations between  $A_n$  and  $g_s$  also revealed higher responsiveness of coffee photosynthesis to changes in stomatal aperture under  $e[\text{CO}_2]$  as compared with  $a[\text{CO}_2]$ , mainly in L2 and L3 canopy layers (Fig. 5B). In other words, our data indicated that coffee plants are able to fix more  $\text{CO}_2$  for a given change in stomatal aperture under  $e[\text{CO}_2]$ , which is probably associated

with higher carboxylation activity. This means that RuBisCO is not  $\text{CO}_2$  saturated in coffee leaves even under  $200 \mu\text{L CO}_2 \text{ L}^{-1}$  above the current air  $[\text{CO}_2]$ . Another interesting point is that the RuBisCO concentration in leaves tends to decrease after long-term exposure to  $e[\text{CO}_2]$ , with photosynthesis being downregulated (Drake *et al.*, 1997). However, no downregulation of photosynthesis was found in coffee trees after several years under  $e[\text{CO}_2]$  (Fig. 3), following similar responses in young coffee trees (Ramalho *et al.*, 2013; Ghini *et al.*, 2015).

Our results also clearly show that increases in water-use efficiency of coffee plants (Fig. 4D–F) were driven by higher photosynthesis rather than lower  $g_s$  or transpiration (Fig. 2; Supplementary Data Fig. S2). Elevated air  $[\text{CO}_2]$  is known to cause stomatal closure in young coffee plants (DaMatta *et al.*, 2016), which was not confirmed in field-grown coffee trees under long-term exposure to air  $[\text{CO}_2]$  enrichment (Fig. 3D–F).

#### Compensation between structural and functional changes under high air $[\text{CO}_2]$

During the fourth reduced growth period under  $e[\text{CO}_2]$ , our estimations showed that Arabica coffee trees presented a significant reduction in LA in the bottom and upper canopy layers, and lower investment in all second-order axes plus third-order axes in lower layers. Those plants also invested more in newly formed third- and fifth-order structures and showed a gradient in photosynthetic responses over the plant vertical profile, with enhancement of light-saturated photosynthesis in sun leaves rather than in shade leaves. In addition, plants showed the ability to cope successfully with such a new environmental scenario, continuing to respond to  $e[\text{CO}_2]$  by structural and functional integration from the metamer (leaf) to the whole-plant scale.

Under elevated air  $[\text{CO}_2]$  and drought events, coffee plants have developed strategies that allowed the maintenance of structural and functional traits, with high leaf assimilation, large investments in new higher axes structures (third- to fifth-order) and probably fine-root turnover as manifested in many tree species (Iversen *et al.*, 2008). In fact, coffee plants show architectural and functional variations from one cycle to another (DaMatta *et al.*, 2007), as revealed by the comparison of results obtained during the initial 2 years of growth (Ghini *et al.*, 2015; DaMatta *et al.*, 2016) with ours taken in the fourth year. The most important modifications when comparing short- and long-term responses to  $e[\text{CO}_2]$  were related to the canopy structure and  $g_s$ , suggesting that structural and functional responses should also be evaluated after long-term exposure in order to obtain a general pattern of response to future environmental scenarios. From a photosynthetic point of view, our data at the whole-plant level showed that changes in plant structure (reduced leaf area) were compensated by changes in plant functioning (increases in photosynthetic rate per unit leaf area in the middle and upper part of the canopy) of coffee trees under free air  $\text{CO}_2$  enrichment.

#### Final remarks

Previous studies have shown that plant responses to  $e[\text{CO}_2]$  are species and even cultivar dependent, and affected by

exposure time (short- and long-term experiments) and experimental strategy (potted vs. field-grown plants). The analytical approach is an additional issue when assessing integration of structural and functional plant responses to e[CO<sub>2</sub>]. Herein, we measured the architectural properties of five axis orders over the whole plant vertical profile and not only the second-order axes at the middle canopy layer of plants, as is usual when evaluating coffee physiology and morphology. The analyses of leaf gas exchange also considered canopy layers, which revealed differential responses to e[CO<sub>2</sub>] in shaded leaves and those exposed to full sunlight.

As a new finding, Arabica coffee plants showed some species-specific responses to CO<sub>2</sub> after growing for 4 years under FACE. In addition to LA, some structural elements were negatively affected by e[CO<sub>2</sub>], such as length and diameter of the second-order axes. From a broad perspective, structural changes under e[CO<sub>2</sub>] may represent a strategy to invest more in new axes over the plant structure, especially considering the third-order axes in the upper canopy layer. Coffee trees maintained a higher *g<sub>s</sub>* and high photosynthesis in the middle and upper canopy layers, which is a very specific response to elevated air [CO<sub>2</sub>]. Downregulation of photosynthesis after long-term exposure to e[CO<sub>2</sub>] was not found, with increased photosynthesis being the key factor leading to high water-use efficiency in coffee trees under FACE. Our findings revealed that one should consider and integrate both structural and functional responses when studying the potential impacts of elevated air [CO<sub>2</sub>] on perennial species.

#### SUPPLEMENTARY DATA

Supplementary data are available online at <https://academic.oup.com/aob> and consist of the following. Figure S1: diagram of axis orders, from the orthotropic axis (O1) to the plagiotropic second to third-order axes (O2–O3), and botanical scales of coding (plant, axes and metamers) in *Coffea arabica*. Figure S2: light response curves of leaf transpiration in field-grown coffee trees under actual and elevated air CO<sub>2</sub> concentrations.

#### ACKNOWLEDGEMENTS

This work was supported by Consórcio Brasileiro de Pesquisa e Desenvolvimento do Café, Brazil [grant no. 02.13.02.042.00.00]. M.R. thanks the Consórcio Pesquisa Café for a fellowship granted, and R.V.R. acknowledges the fellowship granted by the National Council of Scientific and Technological Development (CNPq, Brazil). We thank Rémy Ferrandes, Cristina Sales, Melissa de Martino and Marcela Miranda for technical support during field evaluations, and Jonas Barbosa Tosti for technical laboratory support.

#### LITERATURE CITED

- Adam B, Dones N, Sinoquet H. 2006. *VegeSTAR: software qui calcule l'interception lumineuse et la photosynthèse, version 3.2*. Clermont-Ferrand: INRA.
- Ainsworth EA, Rogers A. 2007. The response of photosynthesis and stomatal conductance to rising [CO<sub>2</sub>]: mechanisms and environmental interactions. *Plant, Cell and Environment* **30**: 258–270.
- Araújo WL, Dias PC, Moraes GA, et al. 2008. Limitations to photosynthesis in coffee leaves from different canopy positions. *Plant Physiology and Biochemistry* **46**: 884–890.
- ASTM. 2000. *Standard test methods for moisture, ash and organic matter of peat and other organic soils, method ASTM D2974-00*. ASTM International.
- Batista ER. 2015. *Respostas fisiológicas e metabólicas de duas cultivares de Coffea arabica L. submetidas a atmosferas enriquecidas em CO<sub>2</sub> em câmaras de topo aberto e sistema FACE*. PhD thesis, São Paulo, Brazil: Instituto de Botânica da Secretaria do Meio Ambiente.
- Battipaglia G, Saurer M, Cherubini P, et al. 2013. Elevated CO<sub>2</sub> increases tree-level intrinsic water use efficiency: insights from carbon and oxygen isotope analyses in tree rings across three forest FACE sites. *New Phytologist* **197**: 544–554.
- Bishop KA, Betzelberger AM, Long SP, Ainsworth EA. 2015. Is there potential to adapt soybean (*Glycine max* Merr.) to future CO<sub>2</sub>? An analysis of the yield response of 18 genotypes in free-air CO<sub>2</sub> enrichment. *Plant, Cell and Environment* **38**: 1765–1774.
- Bunce JA. 2001. Direct and acclimatory responses of stomatal conductance to elevated carbon dioxide in four herbaceous crop species in the field. *Global Change Biology* **7**: 323–331.
- Bunce JA. 2017. Using FACE systems to screen wheat cultivars for yield increases at elevated CO<sub>2</sub>. *Agronomy* **7**: 20. doi: 10.3390/agronomy7010020.
- Camargo AP, Camargo MBP. 2001. Definição e esquematização das fases fenológicas do café arábica nas condições tropicais do Brasil. *Bragantia* **60**: 65–68.
- Carmo-Silva E, Scales JC, Madgwick PJ, Parry MAJ. 2015. Optimizing Rubisco and its regulation for greater resource use efficiency. *Plant, Cell and Environment* **38**: 1817–1832.
- Cavatte PC, Oliveira AA, Morais LE, Martins SC, Sanglard LM, DaMatta FM. 2012. Could shading reduce the negative impacts of drought on coffee? A morphophysiological analysis. *Physiologia Plantarum* **114**: 111–122.
- Cilas C, Bouharmont P, Boccara M, Eskes AB, Baradat PH. 1998. Prediction of genetic value for coffee production in *Coffea arabica* from a half-diallel with lines and hybrids. *Euphytica* **104**: 49–59.
- Correia LE, Alvim CA, Matsunaga FT, Rakocevic M. 2017. Phyllochron, leaf expansion and life span in adult *Coffea arabica* L. plants – impact of branching order, growth intensity period and emitted leaf position. In: *IEEE International Conference on Functional-Structural Plant Growth Modeling, Simulation, Visualization and Applications 2016*, Qingdao, China, 38–43.
- Cousins AB, Adam NR, Wall GW, et al. 2001. Reduced photorespiration and increased energy-use efficiency in young CO<sub>2</sub>-enriched sorghum leaves. *New Phytologist* **150**: 275–284.
- Curtis PS, Wang X. 1998. A meta-analysis of elevated CO<sub>2</sub> effects on woody plant mass, form, and physiology. *Oecologia* **113**: 299–313.
- DaMatta FM, Ronchi CP, Maestri M, Barros RS. 2007. Ecophysiology of coffee growth and production. *Brazilian Journal of Plant Physiology* **19**: 485–510.
- DaMatta FM, Godoy AG, Menezes-Silva PE, et al. 2016. Sustained enhancement of photosynthesis in coffee trees grown under free-air CO<sub>2</sub> enrichment conditions: disentangling the contributions of stomatal, mesophyll, and biochemical limitations. *Journal of Experimental Botany* **67**: 341–352.
- Dengler NG. 1999. Anisophylly and dorsiventral shoot symmetry. *International Journal of Plant Sciences* **160**: 67–80.
- Drake BG, Gonzalez-Mele MA, Long SP. 1997. More efficient plants? A consequence of rising atmospheric CO<sub>2</sub>. *Annual Review of Plant Physiology and Plant Molecular Biology* **48**: 607–637.
- Farquhar GD, von Caemmerer S, Berry JA. 1980. A biochemical model of photosynthetic CO<sub>2</sub> assimilation in leaves of C<sub>3</sub> species. *Planta* **149**: 78–90.
- Ghini R, Torre-Neto A, Dentzien AFM, et al. 2015. Coffee growth, pest and yield responses to free-air CO<sub>2</sub> enrichment. *Climatic Change* **132**: 307–320.
- Gielen B, Calfapietra C, Claus A, Sabatti M, Ceulemans R. 2002. Crown architecture of *Populus* spp. is differentially modified by free-air CO<sub>2</sub> enrichment (POPFACE). *New Phytologist* **153**: 91–99.
- Godin C, Caraglio Y. 1998. A multiscale model of plant topological structures. *Journal of Theoretical Biology* **191**: 1–46 1998.
- Goodfellow J, Eamus D, Duff G. 1997. Diurnal and seasonal changes in the impact of CO<sub>2</sub> enrichment on assimilation, stomatal conductance and growth in a long-term study of *Mangifera indica* in the wet–dry tropics of Australia. *Tree Physiology* **17**: 291–299.

- Griffon S, de Coligny F. 2014.** AMAPstudio: an editing and simulation software suite for plants architecture modeling. *Ecological Modelling* **290**: 3–10.
- van Groenigen KJ, Qi X, Osenberg CW, Luo Y, Hungate BA. 2014.** Faster decomposition under increased atmospheric CO<sub>2</sub> limits soil carbon storage. *Science* **344**: 508–509.
- Hallé F, Oldeman RAA, Tomlinson PB. 1978.** *Tropical trees and forests: an architectural analysis*. Berlin: Springer.
- Herrick JD, Thomas RB. 1999.** Effects of CO<sub>2</sub> enrichment on the photosynthetic light response of sun and shade leaves of canopy sweetgum trees (*Liquidambar styraciflua*) in a forest ecosystem. *Tree Physiology* **19**: 779–786.
- Hillel D, Rosenzweig C. 2012.** Agriculture and environment in a crowding and warming world. In: Hillel D, Rosenzweig C, eds. *Handbook of climate change and agroecosystems: global and regional aspects and implications*. ICP Series on Climate Change Impacts, Adaptation, and Mitigation 2. London: Imperial College Press: 3–10.
- Iversen CM, Ledford J, Norby RJ. 2008.** CO<sub>2</sub> enrichment increases carbon and nitrogen input from fine roots in a deciduous forest. *New Phytologist* **179**: 837–847.
- Jin J, Tang C, Sale P. 2016.** The impact of elevated carbon dioxide on the phosphorus nutrition of plants: a review. *Annals of Botany* **116**: 987–999.
- Jurola E. 2005.** *Photosynthesis, CO<sub>2</sub> and temperature – an approach to analyse the constraints to acclimation of trees to increasing CO<sub>2</sub> concentration*. PhD thesis, Finland: University of Helsinki.
- Kimball BA. 1992.** Cost comparisons among free-air CO<sub>2</sub> enrichment, open-top chamber, and sunlit controlled-environment chamber methods of CO<sub>2</sub> exposure. *Critical Reviews in Plant Sciences* **1**: 265–270.
- Koike T, Watanabe M, Watanabe Y, et al. 2015.** Ecophysiology of deciduous trees native to Northeast Asia grown under FACE (Free Air CO<sub>2</sub> Enrichment). *Journal of Agricultural Meteorology* **71**: 174–184.
- Konrad MLF, Silva JAB, Furlani PR, Machado EC. 2005.** Gas exchange and chlorophyll fluorescence in six coffee cultivars under aluminum stress. *Bragantia* **64**: 339–347.
- Kubiske ME, Zak DR, Pregitzer KS, Takeuchi Y. 2002.** Photosynthetic acclimation of overstory *Populus tremuloides* and understory *Acer saccharum* to elevated atmospheric CO<sub>2</sub> concentration: interactions with shade and soil nitrogen. *Tree Physiology* **22**: 321–329.
- Leakey ADB, Ainsworth EA, Bernacchi CJ, et al. 2009.** Elevated CO<sub>2</sub> effects on plant carbon, nitrogen, and water relations: six important lessons from FACE. *Journal of Experimental Botany* **60**: 2859–2876.
- Long SP, Ainsworth EA, Rogers A, Ort DR. 2004.** Rising atmospheric carbon dioxide: plants face the future. *Annual Review of Plant Biology* **55**: 591–628.
- Macháčová K. 2010.** Open top chamber and free air CO<sub>2</sub> enrichment – approaches to investigate tree responses to elevated CO<sub>2</sub>. *iForest Viterbo* **3**: 102–105.
- Martins LD, Tomaz MA, Lidon FC, DaMatta FM, Ramalho JC. 2014.** Combined effects of elevated [CO<sub>2</sub>] and high temperature on leaf mineral balance in *Coffea* spp. plants. *Climatic Change* **126**: 365–379.
- Martins LD, Silva MJ, Reboledo FH, et al. 2016.** Protective response mechanisms to heat stress in interaction with high [CO<sub>2</sub>] conditions in *Coffea* spp. *Frontiers in Plant Science* **7**: 947. doi: 10.3389/fpls.2016.00947.
- Matsunaga FT, Tosti JB, Androcioli-Filho A, Brancher JD, Costes E, Rakocevic M. 2006.** Strategies to reconstruct 3D *Coffea arabica* L. plant structure. *SpringerPlus* **5**: 2075. doi: 10.1186/s40064-016-3762-4.
- Medlyn BE, Zaehle S, De Kauwe MG, et al. 2015.** Using ecosystem experiments to improve vegetation models. *Nature Climate Change* **5**: 528–534.
- Mot KA. 1990.** Sensing of atmospheric CO<sub>2</sub> by plants. *Plant, Cell and Environment* **13**: 731–737.
- Pradal C, Boudon F, Nouguier C, Chopard J, Godin C. 2008.** PlantGL: A python-based geometric library for 3D plant modelling at different scales. *Graphical Models* **71**: 1–21.
- Prado CHBA, de Moraes JAPV. 1997.** Photosynthetic capacity and specific leaf mass in twenty woody species of Cerrado vegetation under field conditions. *Photosynthetica* **33**: 103–112.
- Pregitzer KS, Zak DR, Curtis PS, et al. 1995.** Atmospheric CO<sub>2</sub>, soil nitrogen and turnover of fine roots. *New Phytologist* **129**: 579–585.
- Rakocevic M, Androcioli-Filho A. 2010.** Morphophysiological characteristics of *Coffea arabica* L in different arrangements: lessons from a 3D virtual plant approach. *Coffee Science* **5**: 154–166.
- Rakocevic M, Marchiori PER, Ferrandes R, Ribeiro RV. 2017.** Estimating the canopy architecture and photosynthesis of *Coffea arabica* L. plants cultivated under long-term elevated air CO<sub>2</sub> concentration. In: *IEEE International Conference on Functional-Structural Plant Growth Modeling, Simulation, Visualization and Applications 2016*, Qingdao, China, 175–182.
- Ramalho JC, Rodrigues AP, Semedo JN, et al. 2013.** Sustained photosynthetic performance of *Coffea* spp. under long-term enhanced [CO<sub>2</sub>]. *PLoS One* **8**: e82712. doi: 10.1371/journal.pone.0082712.
- R Core Team. 2017.** *R: a language and environment for statistical computing*. Vienna, Austria: R Foundation for Statistical Computing, URL <http://www.R-project.org/>
- Reddy KR, Zhao D. 2005.** Interactive effects of elevated CO<sub>2</sub> and potassium deficiency on photosynthesis, growth, and biomass partitioning of cotton. *Field Crops Research* **94**: 201–213.
- Rodrigues WP, Martins MQ, Fortunato AS, et al. 2016a.** Long-term elevated air [CO<sub>2</sub>] strengthens photosynthetic functioning and mitigates the impact of supra-optimal temperatures in tropical *Coffea arabica* and *C. canephora* species. *Global Change Biology* **22**: 415–431.
- Rodrigues WP, Machado Filho JA, Silva JR, et al. 2016b.** Whole-canopy gas exchanges in *Coffea* sp. is affected by supra-optimal temperature and light distribution within the canopy: the insights from an improved multi-chamber system. *Scientia Horticulturae* **211**: 194–202.
- Rodríguez-López N. 2012.** *Ecophysiological acclimation of coffee plant to cope with temporal fluctuations of light supply*. PhD thesis, Brazil: Federal University of Viçosa.
- Ronchi CP, de Almeida WL, Souza DS, Sousa Júnior JM, Guerra AMNM, Pimenta PHC. 2016.** Morphophysiological plasticity of plagiotropic branches in response to change in the coffee plant spacing within rows. *Semina: Ciências Agrárias* **37**: 3819–3834.
- Silva EA, DaMatta FM, Ducatti C, Regazzi AJ, Barros RS. 2004.** Seasonal changes in vegetative growth and photosynthesis of Arabica coffee trees. *Field Crop Research* **89**: 349–357.
- Smith WK, Reed SC, Cleveland CC, et al. 2016.** Large divergence of satellite and Earth system model estimates of global terrestrial CO<sub>2</sub> fertilization. *Nature Climate Change* **6**: 306–312.
- Sreeharsha RV, Sekhar KM, Reddy AR. 2015.** Delayed flowering is associated with lack of photosynthetic acclimation in Pigeon pea (*Cajanus cajan* L.) grown under elevated CO<sub>2</sub>. *Plant Science* **231**: 82–93.
- Tron S, Bodner G, Laio F, Ridolfi L, Leitner D. 2015.** Can diversity in root architecture explain plant water use efficiency? A modeling study. *Ecological Modelling* **312**: 200–210.
- Taba Z, Lichtenthaler HK. 2007.** Long-term acclimation of plants to elevated CO<sub>2</sub> and its interaction with stresses. *Annals of the New York Academy of Sciences* **113**: 135–146.
- Vidal TA, Rossi P, Nechet KL, Ramos NP. 2015.** Impacto do aumento da concentração de dióxido de carbono sobre a decomposição de resíduos culturais. In: *9º Congresso Interinstitucional de Iniciação Científica*, Campinas-SP, Brazil: 1–8.
- Vos J, Evers JB, Buck-Sorlin GH, Andrieu B, Chelle M, de Visser PHB. 2009.** Functional-structural plant modelling: a new versatile tool in crop science. *Journal of Experimental Botany* **61**: 2101–2115.
- Xu Z, Jiang Y, Jia B, Zhou G. 2016.** Elevated-CO<sub>2</sub> response of stomata and its dependence on environmental factors. *Frontiers in Plant Science* **7**: e657. doi: 10.3389/fpls.2016.00657.